

First measurement of the muon magnetic anomaly at Fermilab

Alberto Lusiani, for the FNAL Muon $g-2$ collaboration
Scuola Normale Superiore and INFN, sezione di Pisa

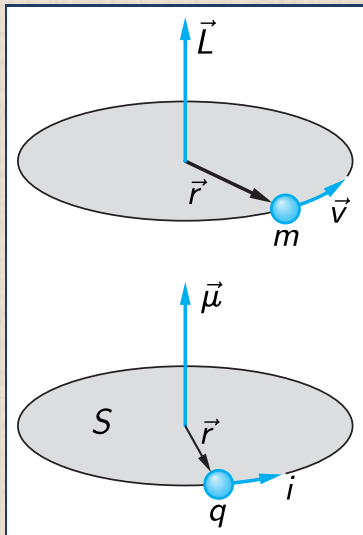


SCUOLA
NORMALE
SUPERIORE



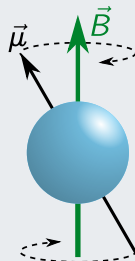
Colloquium
9 June 2021

Magnetic momentum

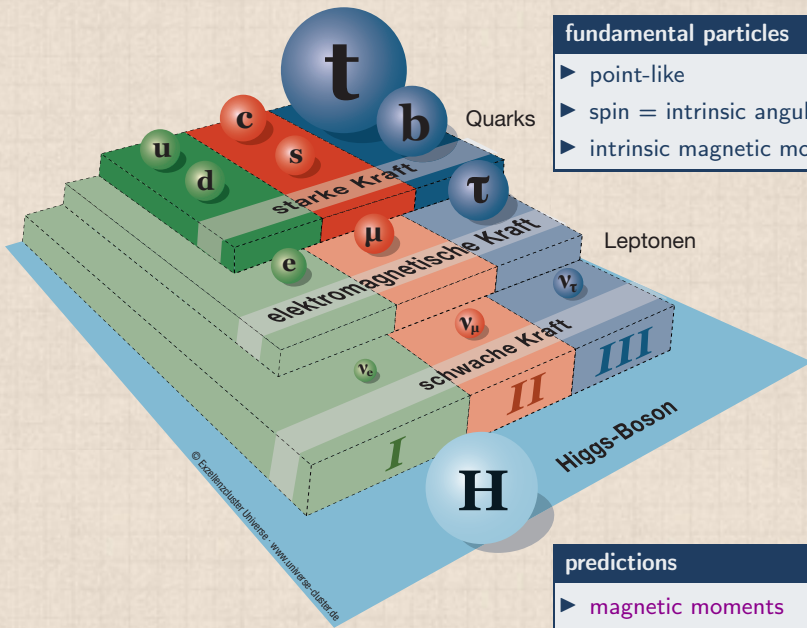


- ▶ $i = \frac{q}{T} = q \frac{v}{2\pi r}$
- ▶ $\mu = iS = q \frac{v}{2\pi r} \pi r^2 = \frac{q}{2} r \frac{mv}{m} = \frac{q}{2m} L$
- ▶ $\vec{\mu} = \frac{q}{2m} \vec{L}$

precession of magnetic momentum in magnetic field



Standard model of particle physics



fundamental particles

- ▶ point-like
- ▶ spin = intrinsic angular momentum
- ▶ intrinsic magnetic momentum

model parameters

- ▶ masses (Higgs couplings)
- ▶ spins
- ▶ charges
- ▶ coupling constants

predictions

- ▶ magnetic moments

Some notation

particle x such as a muon, electron, proton, neutron

- ▶ **magnetic moment** $\vec{\mu}_x = g_x \frac{e}{2m_x} \vec{S}_x$, e = absolute value of electron charge (used also for neutron)
 \vec{S}_x = spin (particle intrinsic angular momentum)
 g_x = **gyromagnetic ratio** (defined also for neutral particles)
- ▶ classical charge distribution: $\rho_q/\rho_m = \text{constant} \Rightarrow g = 1$

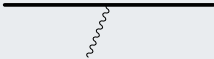
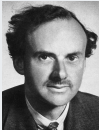
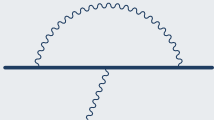




leptons (electron, muon, tau): spin 1/2 fundamental point-like particles

- ▶ $g_e, g_\mu, g_\tau = 2$ at first order and for Dirac equation (note: negative sign omitted for simplicity)
- ▶ $g_e, g_\mu, g_\tau > 2$ including effects of virtual particles exchanges
- ▶ $a_x = \frac{g_x - 2}{2}$ **anomalous gyromagnetic ratio** or **magnetic anomaly**
- ▶ Standard Model precisely predicts g_x, a_x

proton, neutron

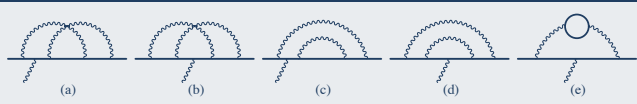
- ▶ $g_p \simeq 5.6, g_n \simeq -3.8$
- ▶ composite particles made of three quarks (mainly interacting with strong force)
- ▶ no precise Standard Model prediction of their magnetic moments
- ▶ strong force interactions are non-perturbative at low energy and difficult to compute

Contributions to a_μ : QED

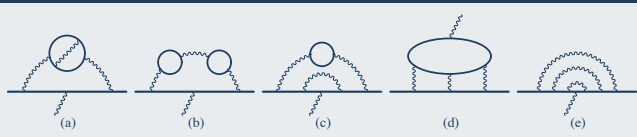
	a_μ contribution [10^{-11}]		order		main authors
	0	± 0	0th	$(g_\mu=2)$	 P. Dirac, 1928
	116 140 973.233	± 0.028	1th	$\frac{\alpha_{\text{QED}}}{2\pi}$	 
	413 217.6252	± 0.0070	2nd		E. Remiddi <i>et al.</i>
	30 141.90226	± 0.00033	3rd		 T. Kinoshita <i>et al.</i>
	381.004	± 0.017	4th		
	5.0783	± 0.0059	5th		

Contributions to a_μ : QED graphs

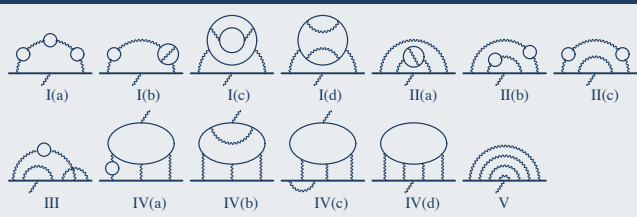
2nd order graphs



3th order graph

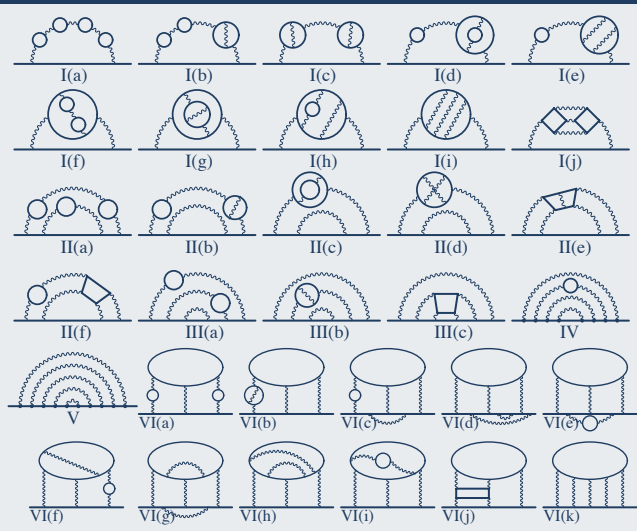


4th order graphs



Contributions to a_μ : QED graphs

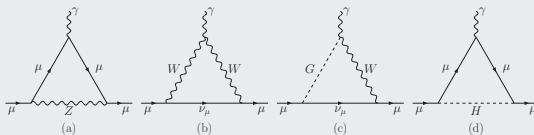
5th order graphs (12672)



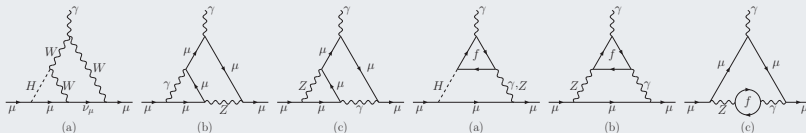
Contributions to a_μ : EW

a_μ contribution $\times 10^{11}$	order
153.6 ± 0.1	1st + 2nd



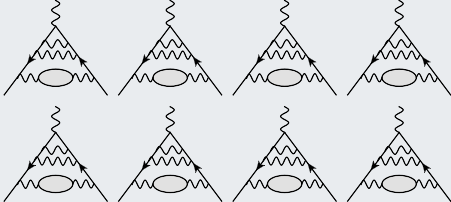
EW graphs, 1st order



EW graphs, 2nd order



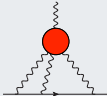
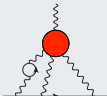
Contributions to a_μ : QCD HVP (hadronic vacuum polarization)

	a_μ contribution [10^{-11}]	order
	6931 ± 40	HLO HVP
	-98.3 ± 7	HNLO HVP
	12.4 ± 1	HNNLO HVP

terminology

LO = "leading order", NLO = "next to leading order", NNLO = "next to next to leading order"

Contributions to a_μ : QCD HLbL (hadronic light-by-light)

	a_μ contribution [10^{-11}]	order
	92 ± 19	HNLO HLbL
	2 ± 1	HNNLO HLbL

Status of a_μ theory prediction work since 1928 updated in December 2020Muon $g-2$ theory initiative group

- ▶ large group of physicists worked from 2017 to 2020 to refine a consensus prediction for a_μ
- ▶ [doi:10.1016/j.physrep.2020.07.006](https://doi.org/10.1016/j.physrep.2020.07.006)

Contribution	Section	Equation	Value $\times 10^{11}$	References
Experiment (E821)		Eq. (8.13)	116 592 089(63)	Ref. [1]
HVP LO (e^+e^-)	Sec. 2.3.7	Eq. (2.33)	6931(40)	Refs. [2–7]
HVP NLO (e^+e^-)	Sec. 2.3.8	Eq. (2.34)	-98.3(7)	Ref. [7]
HVP NNLO (e^+e^-)	Sec. 2.3.8	Eq. (2.35)	12.4(1)	Ref. [8]
HVP LO (lattice, $udsc$)	Sec. 3.5.1	Eq. (3.49)	7116(184)	Refs. [9–17]
HLbL (phenomenology)	Sec. 4.9.4	Eq. (4.92)	92(19)	Refs. [18–30]
HLbL NLO (phenomenology)	Sec. 4.8	Eq. (4.91)	2(1)	Ref. [31]
HLbL (lattice, uds)	Sec. 5.7	Eq. (5.49)	79(35)	Ref. [32]
HLbL (phenomenology + lattice)	Sec. 8	Eq. (8.10)	90(17)	Refs. [18–30, 32]
QED	Sec. 6.5	Eq. (6.30)	116 584 718.931(104)	Refs. [33, 34]
Electroweak	Sec. 7.4	Eq. (7.16)	153.6(1.0)	Refs. [35, 36]
HVP (e^+e^- , LO + NLO + NNLO)	Sec. 8	Eq. (8.5)	6845(40)	Refs. [2–8]
HLbL (phenomenology + lattice + NLO)	Sec. 8	Eq. (8.11)	92(18)	Refs. [18–32]
Total SM Value	Sec. 8	Eq. (8.12)	116 591 810(43)	Refs. [2–8, 18–24, 31–36]
Difference: $\Delta a_\mu := a_\mu^{\text{exp}} - a_\mu^{\text{SM}}$	Sec. 8	Eq. (8.14)	279(76)	

Muon $g-2$ theory initiative collaborators (132), Seattle, Sep 2019



a_μ theory prediction uncertainty is $\Delta a_\mu/a_\mu = 0.37$ ppm

	contributions	uncertainty [ppm]
QED	complete calculation to 5th order	0.001
EW	calculation to NLO	0.010
QCD	primarily non-perturbative	
- HVP	up to NNLO, primarily dispersive	0.340
- HLbL	up to NLO, dispersive + lattice QCD	0.150
total		0.370

dominant QCD contributions uncertainties

First g_μ measurement (1957)

motivation: confirm Lee & Yang predictions about parity violation in pion and muon decay

Observations of the Failure of Conservation of Parity and Charge Conjugation in Meson Decays: the Magnetic Moment of the Free Muon*

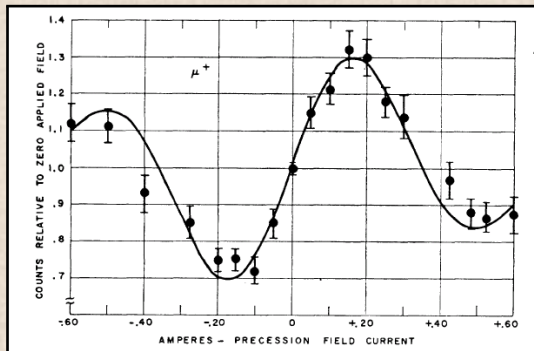
RICHARD L. GARWIN,[†] LEON M. LEDERMAN,
AND MARCEL WEINRICH*Physics Department, Nevis Cyclotron Laboratories,
Columbia University, Irvington-on-Hudson,
New York, New York*

(Received January 15, 1957)

LEE and Yang¹⁻³ have proposed that the long held space-time principles of invariance under charge conjugation, time reversal, and space reflection (parity) are violated by the “weak” interactions responsible for decay of nuclei, mesons, and strange particles. Their hypothesis, born out of the $\tau-\theta$ puzzle,⁴ was accompanied by the suggestion that confirmation should be sought (among other places) in the study of the successive reactions

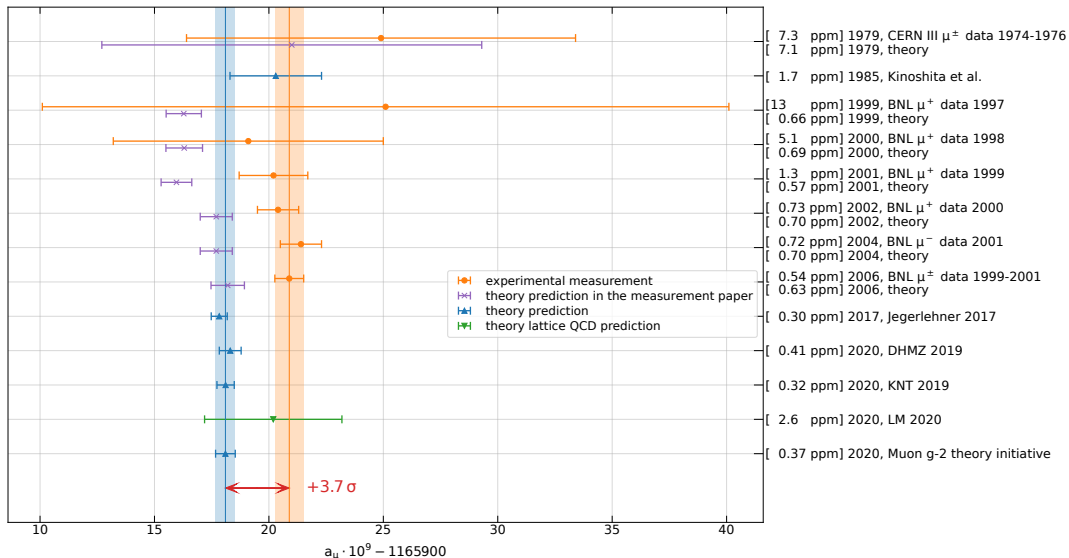
$$\pi^+ \rightarrow \mu^+ + \nu, \quad (1)$$

$$\mu^+ \rightarrow e^+ + 2\nu. \quad (2)$$

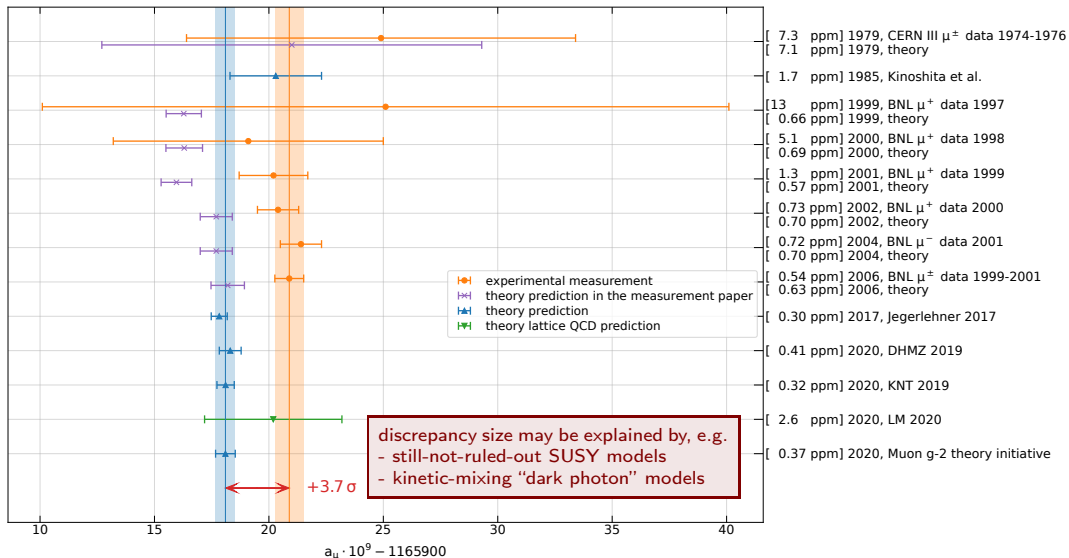


- ▶ forward pion-decay muons are highly polarized
- ▶ μ -decay electrons angular asymmetry vs. μ spin
- ▶ electron rate vs. B field applied to muons
- ▶ $g_\mu = 2.01 \pm 0.01$

a_μ measurements and predictions 1979 – March 2021 (incomplete collection)



a_μ measurements and predictions 1979 – March 2021 (incomplete collection)



a_μ Standard Model test more powerful than a_e for high energy New Physics

a_μ test $\sim 2000\times$ less precise than a_e test
for experimental and theory uncertainties

$$\frac{\Delta(a_\mu^{\text{exp}} - a_\mu^{\text{th}})}{\Delta(a_e^{\text{exp}} - a_e^{\text{th}})} \sim 2000$$

but

a_μ test $\sim 43000\times$ more sensitive than a_e test
for “typical” high-energy New Physics models

$$\frac{a_\mu^{\text{New Physics}}}{a_e^{\text{New Physics}}} \sim \frac{m_\mu^2}{m_e^2} \simeq 43000$$

experiment and theory uncertainties contributions to a_μ test as of March 2021

	δa_μ [ppm]	δa_e [ppb]
experiment	0.54	0.24
theory	0.37	0.20
- α_{QED}	0.00	0.20
- QED	0.00	0.01
- EW	0.01	0.00
- QCD	0.37	0.01
- HVP	0.34	
- HLbL	0.15	

► note: using less precise α_{QED} (Cs 2018) because of inconsistency with α_{QED} (Rb 2020)

Motion and spin precession of muon in uniform magnetic field

muon spin precession relative to momentum

$$\omega_s - \omega_c = \omega_a$$

$$-g_\mu \frac{eB}{2m_\mu} - (1-\gamma) \frac{eB}{m_\mu \gamma} - \left[-\frac{eB}{m_\mu \gamma} \right] = \left[-a_\mu \frac{eB}{m_\mu} \right]$$

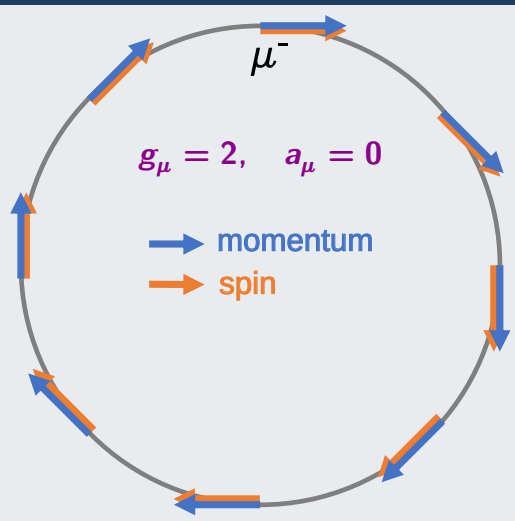
Larmor + Thomas
precessions

cyclotron
frequency

no γ !

- ▶ frequency measurements best for precision
- ▶ magnetic field NMR measurement also frequency
- ▶ angle between momentum and spin $\theta(t) = \omega_a t$

polarized muons in magnetic storage ring



Motion and spin precession of muon in uniform magnetic field

muon spin precession relative to momentum

$$\omega_s - \omega_c = \omega_a$$

$$-g_\mu \frac{eB}{2m_\mu} - (1-\gamma) \frac{eB}{m_\mu \gamma} - \left[-\frac{eB}{m_\mu \gamma} \right] = \left[-a_\mu \frac{eB}{m_\mu} \right]$$

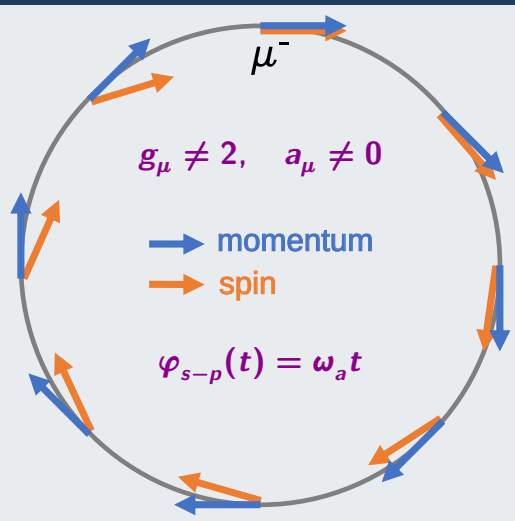
Larmor + Thomas
precessions

cyclotron
frequency

no γ !

- ▶ frequency measurements best for precision
- ▶ magnetic field NMR measurement also frequency
- ▶ angle between momentum and spin $\theta(t) = \omega_a t$

polarized muons in magnetic storage ring



Focusing electric field and magic energy

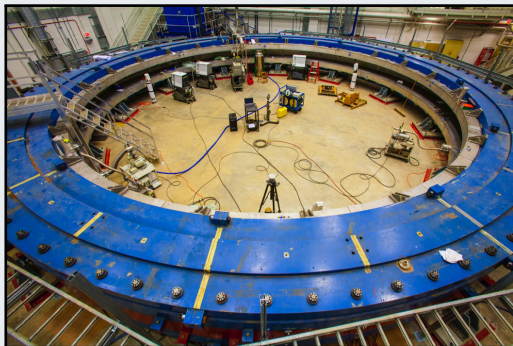
in presence of (focusing) electric field and motion not perfectly transverse to magnetic field

$$\vec{\omega}_a = -\frac{e}{m_\mu} \left[a_\mu \vec{B} - \left(a_\mu - \frac{1}{\gamma^2 - 1} \right) (\vec{\beta} \times \vec{E}) - a_\mu \frac{\gamma}{\gamma + 1} (\vec{\beta} \cdot \vec{B}) \vec{\beta} \right]$$

CERN 1975-, BNL, FNAL

$$p_\mu^{\text{magic}} = 3.094 \text{ GeV} \Rightarrow \gamma = 29.3$$

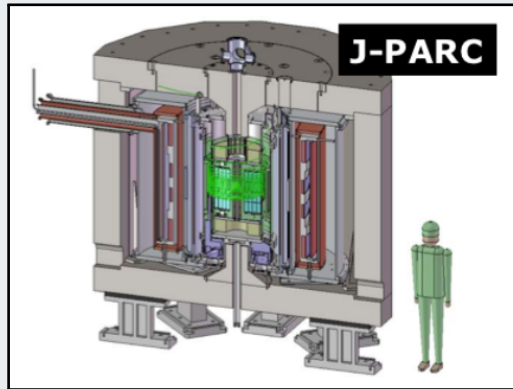
$$\Rightarrow \left(a_\mu - \frac{1}{\gamma^2 - 1} \right) \simeq 0$$



J-PARC E34

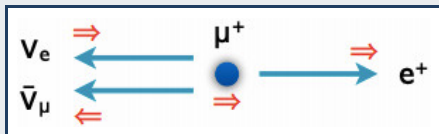
ultra-cold muons

$$E = 0 \Rightarrow \vec{\beta} \times \vec{E} = 0$$



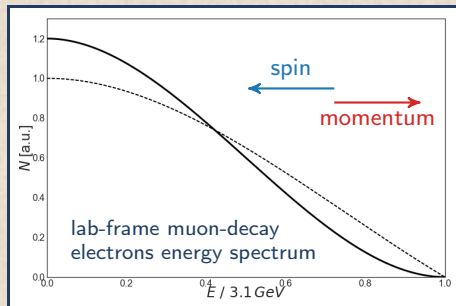
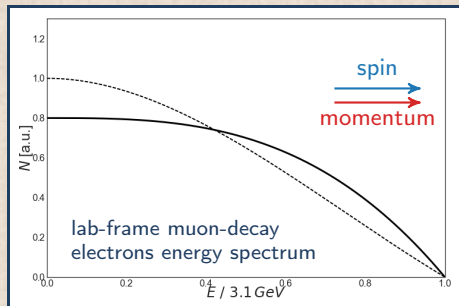
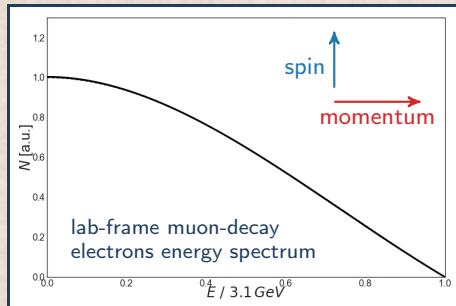
Rate of high-energy muon-decay electrons modulated with $\cos \omega_a t$

- ▶ because of parity violation in muon decay, decay electrons peak along muon spin



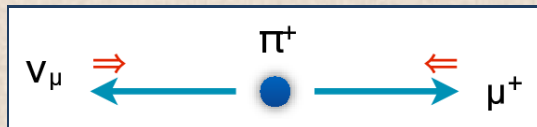
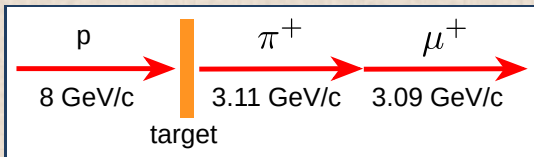
- ▶ electrons decaying along muon momentum have highest energy in laboratory frame

$$N_e(E_e > E_t) = N_{e0} e^{-t/\tau_\mu} (1 + A \cos \omega_a t)$$



Production of polarized muons

- ▶ dump 8 GeV protons on target to produce pions
- ▶ select pions with momentum $p \simeq 3.11$ GeV
- ▶ let them decay into muons
- ▶ in pion rest frame, because of parity violation in pion decay, μ^- spin is aligned with momentum (μ^+ spin is anti-aligned with momentum)
- ▶ in laboratory frame, highest energy muons are $>90\%$ polarized



- ▶ with 8 GeV protons on target, μ^+ are produced $\sim 4\times$ more frequently than μ^-

a_μ measurement: how sub-ppm precision can be obtained

measurement of magnetic field: ω_p

▶ proton spin precession frequency measures magnetic field (NMR): $\hbar\omega_p = 2\mu_p B$

measurements

▶ $\omega_a = a_\mu \frac{eB}{m_\mu}$, $\hbar\omega_p = 2\mu_p B$

spin 1/2 particle $x = \text{proton, muon}$

▶ $S_x = \frac{\hbar}{2}$, $\mu_x = g_x \frac{e}{m_x} S_x$, $a_x = \frac{g_x - 2}{2}$

$$a_\mu = \frac{\omega_a / \omega_p}{\mu_\mu / \mu_p - \omega_a / \omega_p}$$

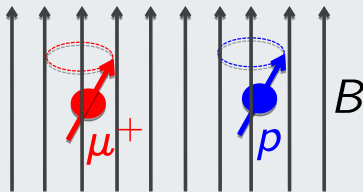
muonium & hydrogen hyperfine transitions



mainly [LAMPF 1999 experiment](#)
precision on CODATA 2018 fit: 22 ppb

actually, best a_μ obtained by adding ω_a / ω_p measurement to Fundamental Physical Constants CODATA fit

ω_a & ω_p in same magnetic field



a_μ experimental precision

FNAL-E989 design precision, compared to BNL-E821 final report (2006)

	BNL E821	FNAL E989	
ω_a statistical	460 ppb	100 ppb	$\times 21$ detected muon decays ($1.6 \cdot 10^{11}$)
ω_a systematic	210 ppb	70 ppb	faster calorimeter with laser calibration, tracker
ω_p systematic	170 ppb	70 ppb	more uniform B , improve NMR measurement
external measurements	negligible	negligible	
total	540 ppb	140 ppb	

FNAL Muon $g-2$ collaboration



USA

- Boston
- Cornell
- Illinois
- James Madison
- Kentucky
- Massachusetts
- Michigan
- Michigan State
- Mississippi
- North Central
- Northern Illinois
- Regis
- Virginia
- Washington

USA National Labs

- Argonne
- Brookhaven
- Fermilab



China

- Shanghai Jiao Tong



Germany

- Dresden
- Mainz



Italy

- Frascati
- Molise
- Naples
- Pisa
- Roma Tor Vergata
- Trieste
- Udine



Korea

- CAPP/IBS
- KAIST



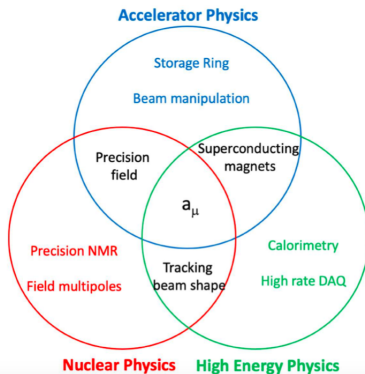
Russia

- Budker/Novosibirsk
- JINR Dubna



United Kingdom

- Lancaster/Cockcroft
- Liverpool
- Manchester
- University College London



~200 collaborators

~40 institutions

7 countries

FNAL Muon $g-2$ collaborators, Elba Island, Spring 2019



BNL storage ring magnet moved to FNAL in 2013 (35 days long trip)



Storage ring magnet adjusted for maximum uniformity

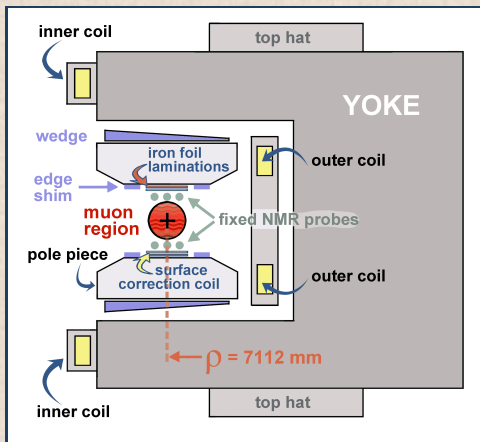
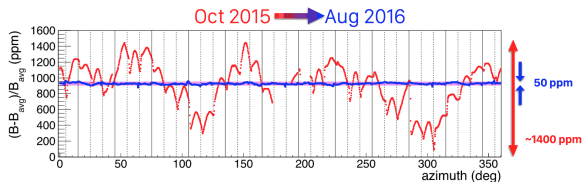
wedging and shimming

- ▶ magnet adjusted to obtain 50 ppm field uniformity
- ▶ 3× better than at BNL

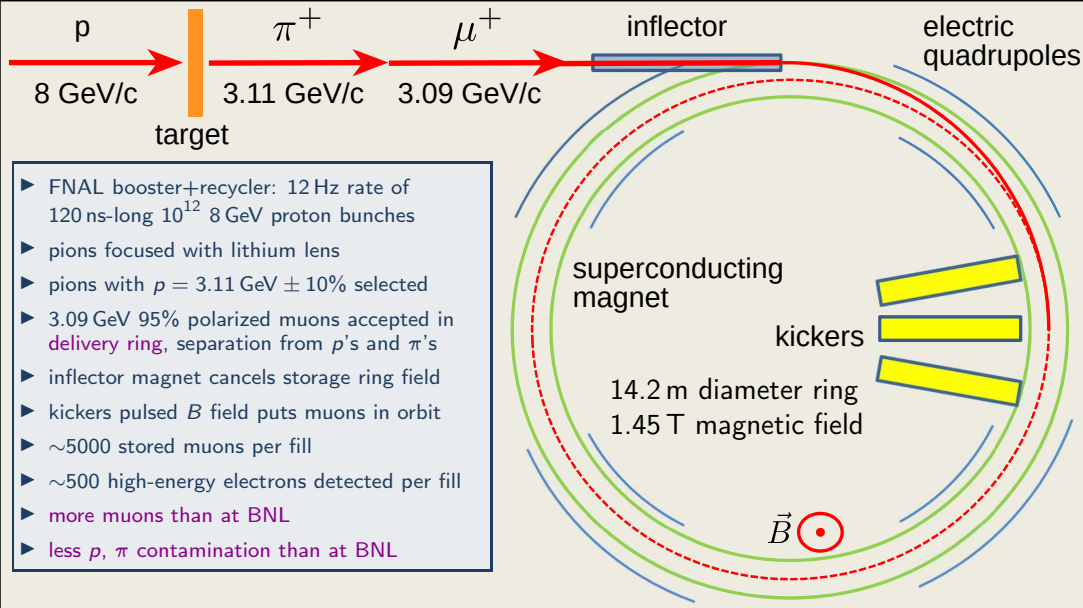
adjustements and insertions

- ▶ 72 poles
- ▶ 864 wedges
- ▶ 24 iron top hats
- ▶ 8000 surface iron foils

magnetic field made uniform to 50 ppm

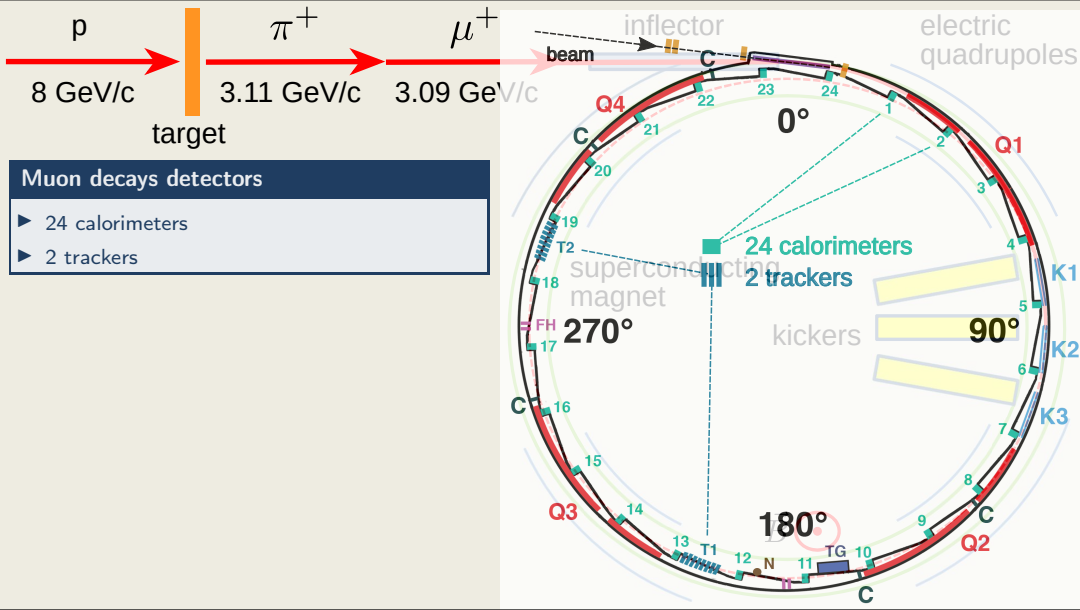


Muon production, storage and decay at FNAL



- ▶ FNAL booster+recycler: 12 Hz rate of 120 ns-long 10^{12} 8 GeV proton bunches
- ▶ pions focused with lithium lens
- ▶ pions with $p = 3.11 \text{ GeV} \pm 10\%$ selected
- ▶ 3.09 GeV 95% polarized muons accepted in **delivery ring**, separation from p 's and π 's
- ▶ inflector magnet cancels storage ring field
- ▶ kickers pulsed B field puts muons in orbit
- ▶ ~ 5000 stored muons per fill
- ▶ ~ 500 high-energy electrons detected per fill
- ▶ **more muons than at BNL**
- ▶ **less p , π contamination than at BNL**

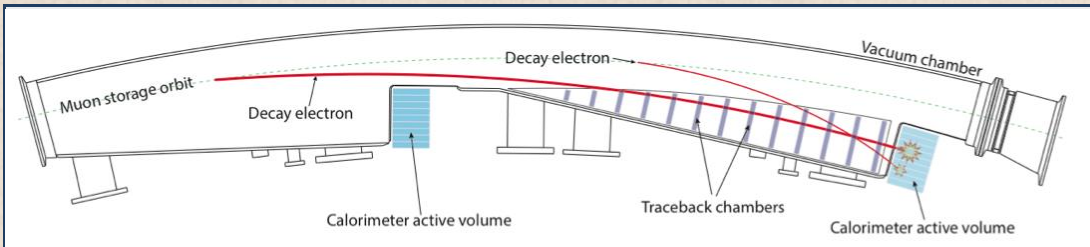
Muon production, storage, decay and detection at FNAL



FNAL-E989 storage ring and detectors



Muon decays detectors



- ▶ **24 calorimeter modules** of 6×9 PbF_2 crystals with 800 MHz-sampling SiPM readout
 - ▶ measure muon-decay electrons energy detecting Cherenkov light
 - ▶ accurate gain monitoring with **laser calibration system**
- ▶ **2 straw chamber trackers** with total of about 1000 channels
 - ▶ reconstruct beam distribution inside storage ring from muon decay electrons

comparison with E821

- ▶ more granular calorimeter, faster data acquisition
- ▶ improved calorimeter gain monitoring
- ▶ improved tracking

Conceptual formula for $R'_\mu(T) = \omega_a / \tilde{\omega}'_p(T)$

$$R'_\mu(T) = \frac{\omega_a}{\tilde{\omega}'_p(T)} \stackrel{\text{conceptually}}{=} \frac{f_{\text{blind}} \omega_a^m (1 + C_e + C_p + C_{\text{ml}} + C_{\text{pa}})}{f_{\text{calib}} \langle \omega'_p(T)(x, y, \varphi) \times M(x, y, \varphi) \rangle (1 + B_k + B_q)}$$

 ω_a measurement and corrections

- ▶ f_{blind} correction for blinding clock offset
- ▶ ω_a^m *measured* precession of muon spin relative to momentum rotation in magnetic field
- ▶ C_e ω_a electric field correction
- ▶ C_p ω_a pitch correction (vertical beam oscillations)
- ▶ C_{ml} ω_a muon loss correction
- ▶ C_{pa} ω_a phase acceptance correction

 $\tilde{\omega}'_p(T)$ measurement and corrections

- ▶ f_{calib} magnetic field probes calibration
- ▶ $\omega'_p(T)(x, y, \varphi)$ measured shielded proton spin precession frequency map in storage ring
- ▶ $M(x, y, \varphi)$ muon beam distribution
- ▶ B_k $\tilde{\omega}'_p(T)$ kicker eddy fields correction
- ▶ B_q $\tilde{\omega}'_p(T)$ electric quadrupoles transient field correction

Multiple analysis groups

 ω_a^m

- ▶ 11 different measurements
- ▶ by 6 analysis groups
- ▶ using 4 different methods to fit rate of muon-decay positrons over time

 $\tilde{\omega}'_p(T)$

- ▶ 2 different measurements
- ▶ by 2 analysis groups
- ▶ using 2 different methods

Run 1 data samples, collected in 2018

muon decays

Dataset	# Days (Apr-Jun 2018)	Tune (n)	Kicker (kV)	# fills [10^4]	# positrons [10^9]
1a	3	0.108	130	151	0.92
1b	7	0.120	137	196	1.28
1c	9	0.120	132	333	1.98
1d	24	0.107	125	733	4.00

total of **8.2 billion positrons** ($\sim 1.2 \times$ BNL), $\sim 6\%$ of E989 goal of $21 \times$ BNL
 4 run periods with different kickers and quadrupoles settings, hence different beam dynamics

magnetic field

magnetic field measurements weighted by detected muon decays

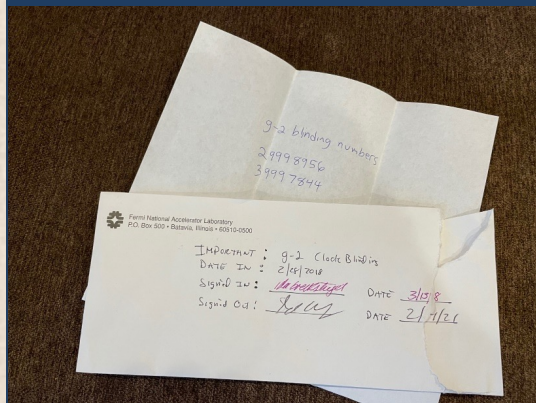
Blinding procedures (f_{blind})

- ▶ 40 MHz base nominal clock used for ω_a data acquisition modified with random ± 25 ppm offset
- ▶ secret offset conserved by two persons that are not members of the collaboration
- ▶ each year of data-taking (Run) is separately blinded
- ▶ second software blinding offset for each of the independent ω_a analysis groups (honor-code based)

blinding of 2018 Run



blinded clock for 2018



Reconstruction of positron energy deposits in calorimeters

readout

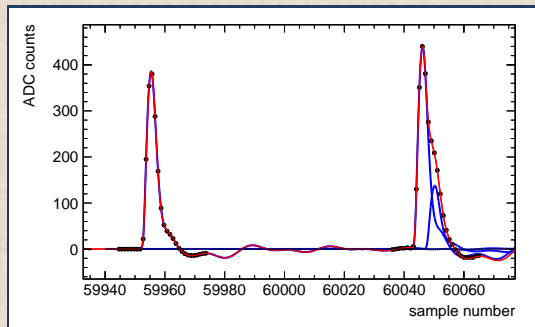
- ▶ record SiPM samples for all deposits > 50 MeV

fit using crystal pulses templates

- ▶ get template pulse for each crystal from data
- ▶ samples fit to one or more superposed templates

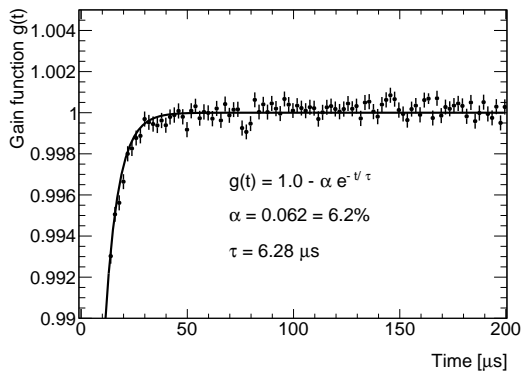
two reconstruction algorithms

- ▶ local: fit individual crystals
- ▶ global: global fit over multiple crystals

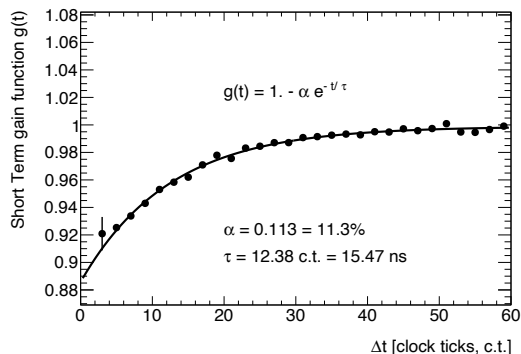


Calorimeter gain variation, measured with laser pulses and corrected

- ▶ SiPM gain is reduced by occurrence of preceding hits
- ▶ gain monitored by reading back reference laser light pulses injected in PbF₂ crystals
- ▶ positron energy measurement from SiPM readout corrected for average measured gain loss

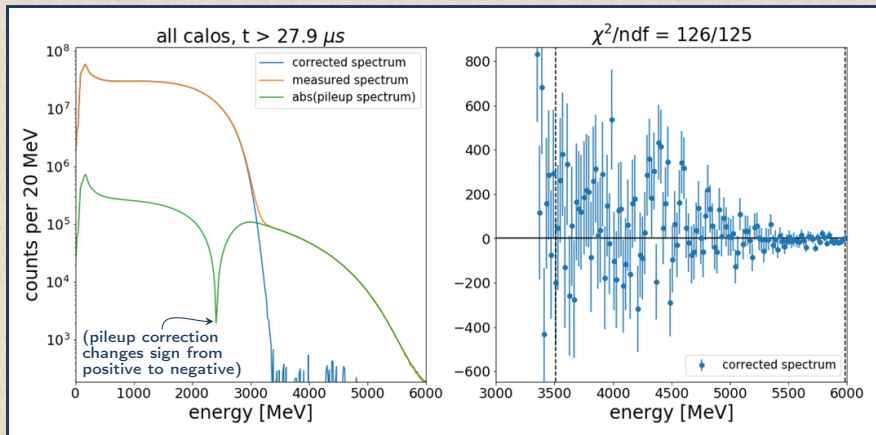
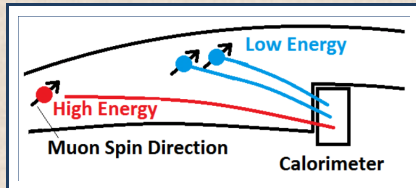
 μ s time scale SiPM power supply recovery time

ns time scale SiPM pixel recovery time



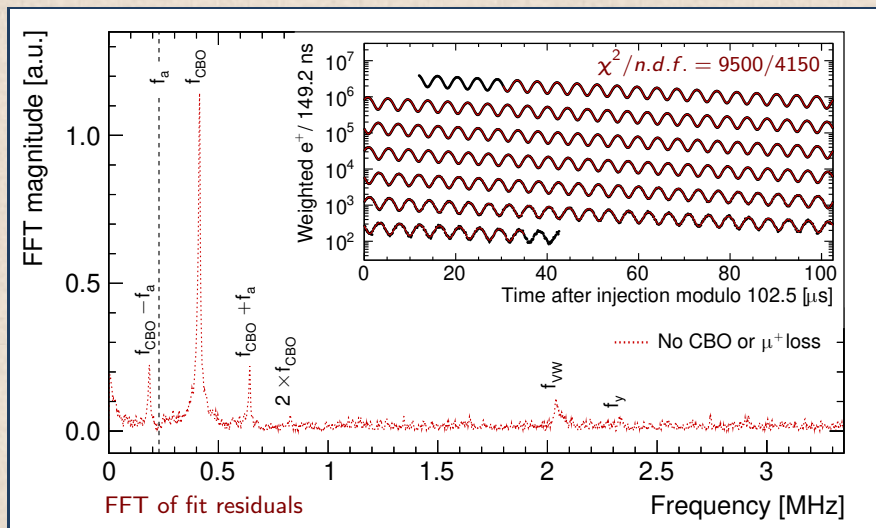
Pileup, statistically subtracted

- ▶ three different methods have been used by 6 analysis groups



Muon precession, 5 parameters ω_a fit model

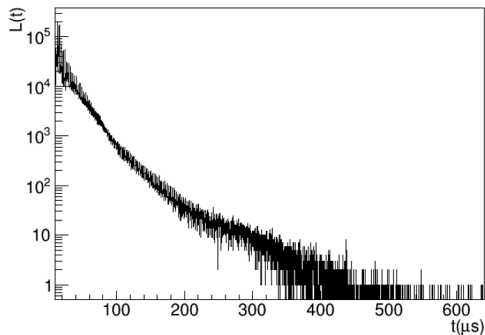
- ▶ number of positron decays with $E > \sim 1.7$ GeV, binned over time, from 30 to 650 μ s
- ▶ fit with $N(t) = N_0 e^{-t/\tau_\mu} [1 + A \cos(\omega_a t + \varphi)]$



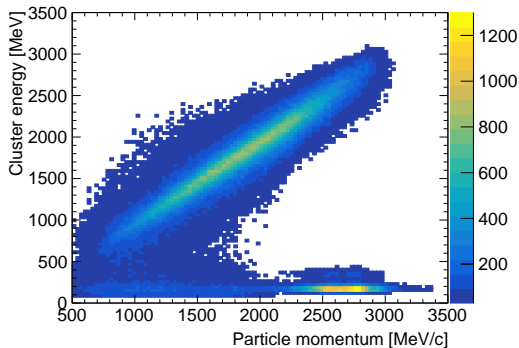
Extend ω_a fit model to account for lost muons on collimators

- ▶ some muons hit collimators and are lost
- ▶ muon loss rate during a fill measured with 3-4-5 coincidences of m.i.p. on calorimeters
- ▶ overall normalization of muon loss included as fit parameter

muon loss vs. time



energy in calorimeter vs. momentum in tracker



Muon precession, 22-parameters ω_a fit

- ▶ include beam dynamics oscillations of beam position and spread
- ▶ include effect of muon loss on collimators

$$N_0 e^{-\frac{t}{\gamma\tau}} (1 + A \cdot A_{BO}(t) \cos(\omega_a t + \varphi + \varphi_{BO}(t))) \cdot N_{CBO}(t) \cdot N_{VW}(t) \cdot N_y(t) \cdot N_{2CBO}(t) \cdot \Lambda(t)$$

$$A_{BO}(t) = 1 + A_A \cos(\omega_{CBO}(t) \cdot t + \varphi_A) e^{-\frac{t}{\tau_{CBO}}}$$

$$\varphi_{BO}(t) = A_\varphi \cos(\omega_{CBO}(t) \cdot t + \varphi_\varphi) e^{-\frac{t}{\tau_{CBO}}}$$

$$N_{CBO}(t) = 1 + A_{CBO} \cos(\omega_{CBO}(t) \cdot t + \varphi_{CBO}) e^{-\frac{t}{\tau_{CBO}}}$$

$$N_{2CBO}(t) = 1 + A_{2CBO} \cos(2\omega_{CBO}(t) \cdot t + \varphi_{2CBO}) e^{-\frac{t}{2\tau_{CBO}}}$$

$$N_{VW}(t) = 1 + A_{VW} \cos(\omega_{VW}(t) \cdot t + \varphi_{VW}) e^{-\frac{t}{\tau_{VW}}}$$

$$N_y(t) = 1 + A_y \cos(\omega_y(t) \cdot t + \varphi_y) e^{-\frac{t}{\tau_y}}$$

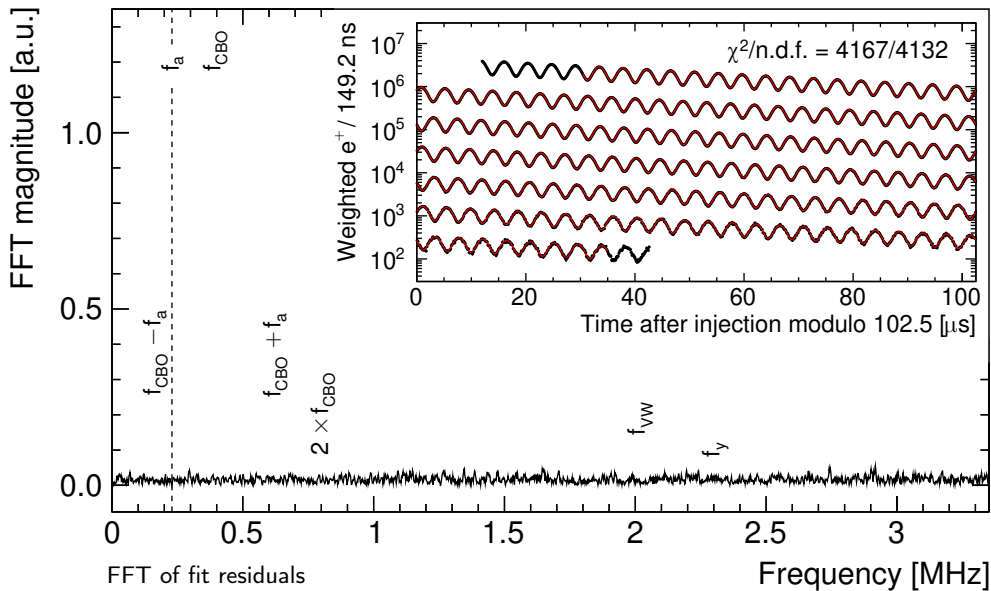
$$\Lambda(t) = 1 - k_{LM} \int_{t_0}^t L(t') e^{t'/\tau} dt'$$

$$\omega_{CBO}(t) = \omega_0^{CBO} + \frac{A}{t} e^{-\frac{t}{\tau_A}} + \frac{B}{t} e^{-\frac{t}{\tau_B}}$$

$$\omega_y(t) = F \omega_{CBO}(t) \sqrt{2\omega_c / F \omega_{CBO}(t) - 1}$$

$$\omega_{VW}(t) = \omega_c - 2\omega_y(t)$$

22 parameters ω_a fit has $\chi^2/n.d.f.$ consistent with 1



6 analysis groups, 4 analysis methods, 11 ω_a fits

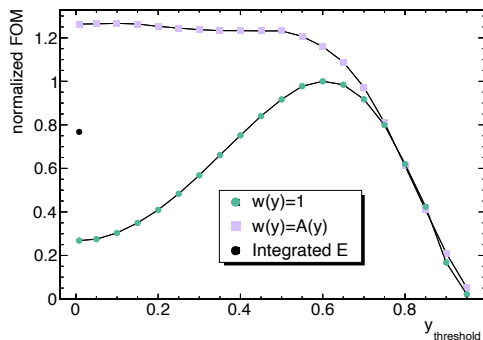
4 analysis methods

- ▶ T (threshold): $\sum N(E_{e^+})$ $E_{e^+} > 1.7$ GeV
- ▶ R (ratio): (see below) $E_{e^+} > 1.7$ GeV
- ▶ A (asymmetry): $\sum A \cdot N(E_{e^+})$ $E_{e^+} > 1.0$ GeV
- ▶ Q (charge): \sum energy deposits no threshold

ratio method

- ▶ randomly split time-binned positron decays in 4 sets
- ▶ displace time of two sets by $\pm T_a/2$
- ▶ ratio of 2 linear combinations can be fitted with just $A \cos(\omega_a t + \varphi)$ (instead of 5-par. fit)

- ▶ two reconstruction algorithms
- ▶ three pileup correction algorithms

FOM vs. E/E_{\max} threshold for T/R, A, Q

R(ω_a) Rn 1 measurement inputs

Run 1a

	CA	EA	SA	NA	CT	ST	ST	ST	ST	ST	
Δ Bias [pph]	-2029.82	-2041.292	-2042.833	-2017.307	-2002.286	-2021.122	-2004.773	-2079.823	-2061.947	-2060.788	-2026.209
val	1261.490	1261.154	1261.600	1261.864	1260.941	1261.277	1261.710	1262.500	1261.011	1260.221	1260.221
stat	129.182	119.710	121.627	119.616	120.644	121.677	120.644	121.677	120.644	121.677	120.644
sys	37.431	120.251	116.165	105.226	98.226	36.173	37.270	98.663	60.427	57.160	50.322
Time randomization need	6.326	26.500	27.900	16.900	20.200	6.714	21.370	22.500	15.500	22.500	15.500
Time correction	0.720	0.000	0.000	0.000	0.000	0.000	0.000	0.000	0.000	0.000	0.000
Classier time assignment	0.000	1.000	1.000	1.000	1.000	1.000	1.000	1.000	1.000	1.000	1.000
Is-fill gain amplitude	4.411	21.431	1.000	14.200	7.790	3.405	23.620	2.500	15.300	7.718	0.000
Is-fill gain time constant	0.000	0.000	0.000	0.000	0.000	0.000	0.000	0.000	0.000	0.000	0.000
STP gain amplitude	0.177	0.049	0.000	2.400	0.091	0.005	0.103	0.000	0.800	0.053	0.000
STP gain time constant	0.000	0.750	0.000	0.000	0.000	0.000	0.146	0.000	0.000	0.000	0.000
Flux covariance matrix	0.000	0.000	0.000	0.000	0.000	0.000	0.000	0.000	0.000	0.000	0.000
Flux phase	0.744	18.211	14.400	13.800	21.700	12.900	17.240	18.200	16.200	10.200	10.200
Flux cluster time model	0.000	0.821	47.000	0.000	5.100	0.000	12.652	0.500	0.400	0.000	0.000
Flux cluster energy model	0.000	7.005	11.000	0.000	1.000	0.000	11.500	0.000	10.900	0.000	0.000
Flux phase error	0.000	0.000	0.000	0.000	0.000	0.000	0.000	0.000	0.000	0.000	0.000
Flux time/energy bias	0.160	0.000	0.000	0.000	0.027	0.000	0.000	0.000	0.000	0.000	0.000
Flux time/energy error	0.003	0.000	0.000	0.000	0.000	0.000	0.000	0.000	0.000	0.000	0.000
Useless piping	0.946	1.100	3.000	10.000	0.800	3.413	5.300	5.400	10.000	0.600	0.000
Triple piping correction	0.000	0.000	0.000	0.000	0.000	0.000	0.000	0.000	0.000	0.000	0.000
Piping simulation	0.000	0.000	0.000	0.000	0.000	0.000	0.000	0.000	0.000	0.000	0.000
Piping artificial dead time	0.000	0.000	0.000	0.000	0.000	0.000	0.000	0.000	0.000	0.000	0.000
Loss covariance matrix	0.000	0.000	0.000	0.000	0.000	0.000	0.000	0.000	0.000	0.000	0.000
Loss time scale	0.000	1.000	0.000	0.200	0.000	0.000	0.200	0.000	0.000	0.000	0.000
Loss energy cuts	0.000	0.000	0.000	0.000	0.000	0.000	0.000	0.000	0.300	0.000	0.000
Loss statistics	1.596	0.000	0.000	0.000	1.522	0.000	0.000	0.000	0.000	0.000	0.000
Loss detection efficiency	1.075	0.000	0.000	0.000	1.062	0.000	0.000	0.000	0.000	0.000	0.000
Fluxed loss scale	0.000	0.000	0.000	0.000	0.000	0.000	0.000	0.000	0.000	0.000	0.000
High-order coincidences	0.000	0.700	0.000	0.000	0.000	0.000	0.700	0.000	0.000	0.000	0.000
CRD frequency change	5.638	11.400	7.100	19.900	10.000	4.299	9.800	5.800	17.300	3.300	5.500
CRD stochastic coverage	24.046	29.700	36.500	38.300	32.524	32.500	47.500	28.500	35.500	41.500	31.500
CRD time constants	4.145	14.200	20.300	11.000	10.000	8.079	2.700	2.000	13.500	10.800	6.000
Flux CRD time constant	0.000	0.000	0.000	0.000	0.000	0.000	0.000	0.000	0.000	0.000	0.000
Vertical drift	0.000	0.000	0.000	0.000	0.000	0.000	0.000	0.000	0.000	0.000	0.000
Non-rotation period	0.000	0.000	0.000	0.000	0.000	0.000	0.000	0.000	0.000	0.000	0.000
Run lifetime	0.000	0.000	0.000	0.000	0.000	0.000	0.000	0.000	0.000	0.000	0.000
Ad hoc correction	5.593	5.000	77.700	27.800	28.700	5.446	13.000	78.000	4.000	23.900	0.000

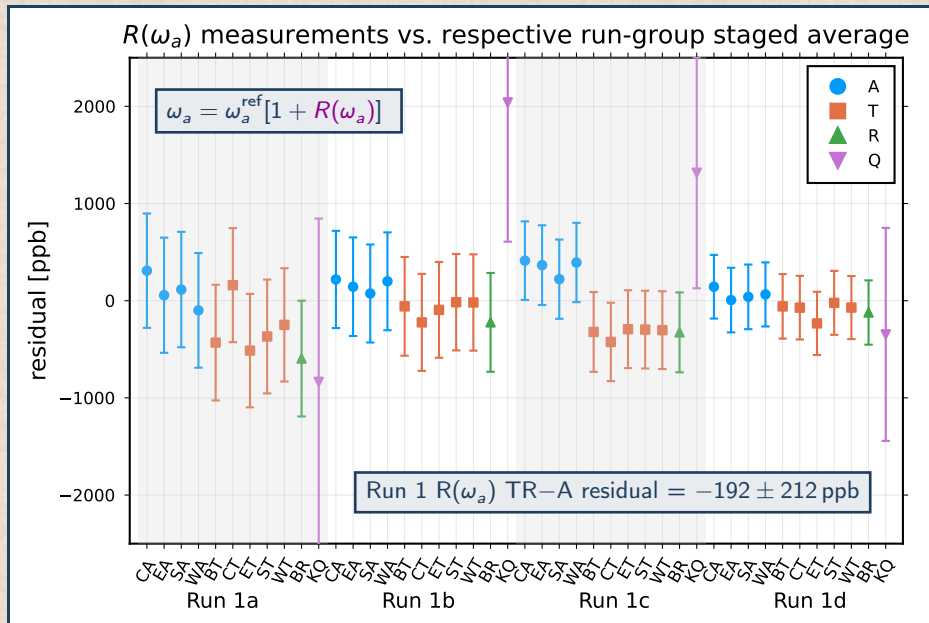
Run 1b

	CA	EA	SA	NA	CT	ST	ST	ST	ST	ST	ST
Δ Bias [pph]	-2046.500	-2701.281	-2701.947	-2696.653	-2704.183	-2729.341	-2700.581	-2701.927	-2704.863	-2709.283	-2696.366
val	1025.180	1018.000	1025.971	1031.843	1107.710	1108.200	1111.900	1109.700	1109.420	1108.464	1109.474
stat	1023.164	1022.104	1023.164	1022.104	1022.104	1022.104	1022.104	1022.104	1022.104	1022.104	1022.104
sys	62.548	110.800	84.960	108.160	60.425	60.425	60.425	60.425	60.425	60.425	60.425
Time randomization need	5.894	23.800	17.100	13.800	15.500	15.500	15.500	15.500	15.500	15.500	15.500
Time correction	1.473	0.000	0.000	0.000	0.000	0.000	0.000	0.000	0.000	0.000	0.000
Classier time assignment	1.000	1.000	1.000	1.000	1.000	1.000	1.000	1.000	1.000	1.000	1.000
Is-fill gain amplitude	3.273	6.475	6.400	20.900	3.282	3.857	6.662	3.500	22.800	0.929	0.000
Is-fill gain time constant	0.000	0.000	0.000	0.000	0.000	0.000	0.000	0.000	0.000	0.000	0.000
STP gain amplitude	0.075	0.089	0.000	0.400	0.042	0.000	0.068	0.000	0.600	0.040	0.000
STP gain time constant	0.000	0.600	0.000	0.000	0.000	0.000	0.000	0.000	0.000	0.000	0.000
Flux covariance matrix	0.000	0.000	0.000	0.000	0.000	0.000	0.000	0.000	0.000	0.000	0.000
Flux phase	0.489	14.533	12.500	12.500	11.400	8.444	10.400	7.000	11.400	7.000	11.400
Flux cluster time model	0.000	64.159	53.000	0.000	4.600	0.000	14.223	7.200	0.000	4.800	0.000
Flux cluster energy model	0.000	0.000	0.000	0.000	0.000	0.000	0.000	0.000	0.000	0.000	0.000
Flux phase error	0.000	0.000	0.000	0.000	0.000	0.000	0.000	0.000	0.000	0.000	0.000
Flux time/energy bias	0.162	0.000	0.000	0.000	0.000	0.000	0.000	0.000	0.000	0.000	0.000
Flux time/energy error	0.017	0.000	0.000	0.000	0.000	0.000	0.000	0.000	0.000	0.000	0.000
Useless piping	2.812	3.900	1.800	10.000	1.300	1.764	3.500	1.800	10.000	0.900	0.000
Triple piping correction	0.000	0.000	0.000	0.000	0.000	0.000	0.000	0.000	0.000	0.000	0.000
Piping simulation	0.000	0.000	0.000	0.000	0.000	0.000	0.000	0.000	0.000	0.000	0.000
Piping artificial dead time	0.000	0.000	0.000	0.000	0.000	0.000	0.000	0.000	0.000	0.000	0.000
Loss covariance matrix	0.000	0.000	0.000	0.000	0.000	0.000	0.000	0.000	0.000	0.000	0.000
Loss time scale	0.000	1.000	0.000	0.100	0.000	0.000	0.100	0.000	0.000	0.000	0.000
Loss energy cuts	0.000	0.000	0.000	0.000	0.000	0.000	0.000	0.000	0.300	0.000	0.000
Loss statistics	0.770	0.000	0.000	0.000	0.000	0.000	0.727	0.000	0.000	0.000	0.000
Loss detection efficiency	0.816	0.000	0.000	0.000	0.800	0.000	0.877	0.000	0.000	0.000	0.000
Fluxed loss scale	0.000	0.000	0.000	0.000	0.000	0.000	0.000	0.000	0.000	0.000	0.000
High-order coincidences	0.000	0.700	0.000	0.000	0.000	0.000	0.000	0.000	0.000	0.000	0.000
CRD frequency change	14.216	12.200	13.500	18.000	22.500	12.135	11.200	11.800	15.900	0.700	16.000
CRD stochastic coverage	2.400	7.000	2.800	15.000	1.700	1.504	12.700	2.500	7.000	1.100	1.000
CRD time constants	41.888	2.000	11.000	45.000	23.100	38.225	3.500	3.000	30.000	21.800	8.000
Flux CRD time constant	0.000	0.000	0.000	0.000	0.000	0.000	0.000	0.000	0.000	0.000	0.000
Vertical drift	0.000	0.000	0.000	0.000	0.000	0.000	0.000	0.000	0.000	0.000	0.000
Non-rotation period	0.000	0.000	0.000	0.000	0.000	0.000	0.000	0.000	0.000	0.000	0.000
Run lifetime	0.000	0.000	0.000	0.000	0.000	0.000	0.000	0.000	0.000	0.000	0.000
Ad hoc correction	18.560	57.000	13.800	37.300	11.800	18.470	33.000	36.000	44.700	13.300	0.000

Run 1c

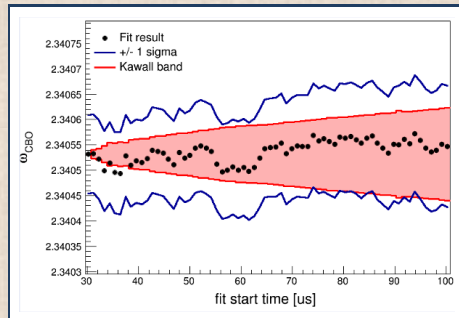
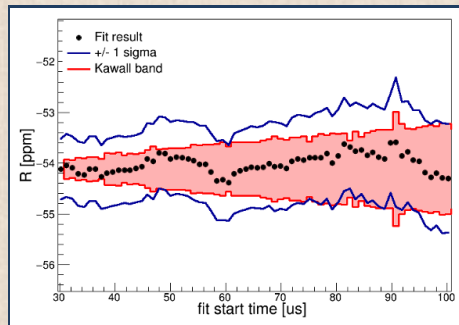
	CA	EA	SA	NA	CT	ST	ST	ST	ST	ST	ST
Δ Bias [pph]	-2753.151	-2759.732	-2744.407	-2772.204	-2767.004	-2802.191	-2788.082	-2785.477	-2798.924	-2792.714	-2629.387
val	823.967	823.967	823.967	823.967	823.967	823.967	823.967	823.967	823.967	823.967	823.967
stat	823.967	823.967	823.967	823.967	823.967	823.967	823.967	823.967	823.967	823.967	823.967
Time randomization need	38.971	38.971	38.971	38.971	38.971	38.971	38.971	38.971	38.971	38.971	38.971
Time correction	1.176	0.000	0.000	0.000	1.142	0.000	0.000	0.000	0.000	0.000	0.000
Classier time assignment	1.000	1.000	1.000	1.000	1.000	1.000	1.000	1.000	1.000	1.000	1.000
Is-fill gain amplitude	2.876	9.986	3.700	13.100	4.129	3.484	9.947	6.000	12.000	1.494	0.000
Is-fill gain time constant	0.000	0.000	0.000	0.000	0.000	0.000	0.000	0.000	0.000	0.000	0.000
STP gain amplitude	0.117	0.217	0.000								

In each of 4 datasets, 11 ω_a measurements are consistent between each-other

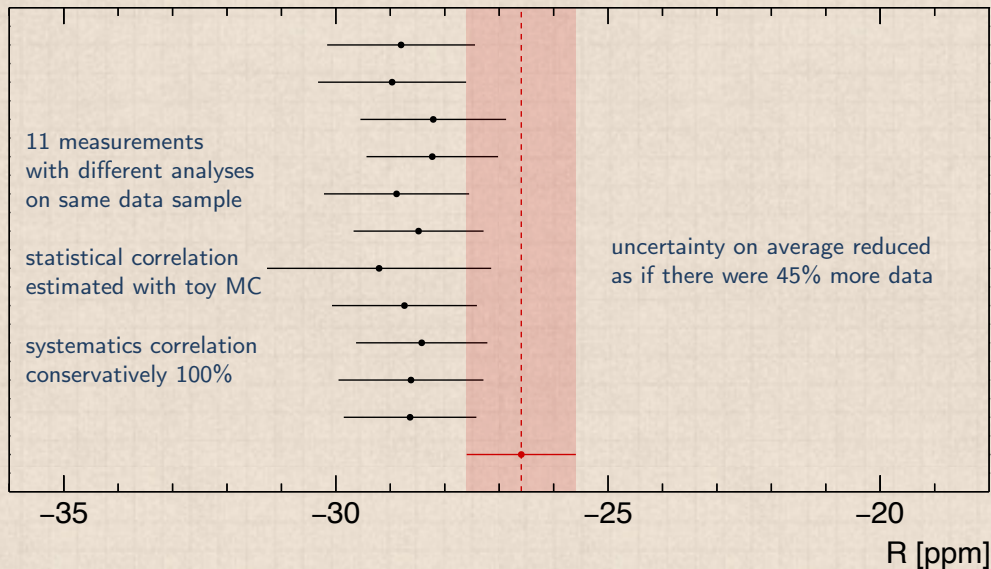


A large number of consistency checks has been completed

- ▶ fit results ought to be stable vs. chosen start time
- ▶ similar checks check performed vs.
 - ▶ calorimeter station
 - ▶ bunch number
 - ▶ Run number
 - ▶ time of day
 - ▶ positron energy bin
 - ▶ position within calorimeter
 - ▶ ...



Average of 11 \sim critically correlated measurements with imprecise correlation



resilient close-to-optimal combination:
 unweighted average of just the 4 A-method measurements (A-method is most precise one)

Early to late effects

- ▶ unaccounted variations of conditions during muon fill time can induce biases on ω_a fit result

example of early-to-late effect: phase variation due to muon loss

- ▶ $N(t) = N_0 e^{-t/\tau_\mu} [1 + A \cos(\omega_a t + \varphi)]$ phase φ = muon spin-momentum angle at injection
- ▶ muon loss depends on momentum \Rightarrow muon sample momentum varies $\bar{p} = \bar{p}(t)$
- ▶ **single muon phase depends on momentum** (because of production chain) $\bar{\varphi} = \bar{\varphi}(\bar{p})$
- ▶ at first order
$$\bar{\varphi}(t) = \bar{\varphi}_0 + \frac{d\bar{\varphi}}{d\bar{p}} \frac{d\bar{p}}{dt} t = \bar{\varphi}_0 + \frac{d\bar{\varphi}}{d\bar{p}} \frac{d\bar{p}}{dt} t \simeq \bar{\varphi}_0 + \bar{\varphi}' t$$
- ▶ muon rate modulation $\cos(\omega_a t + \bar{\varphi}(t)) \simeq \cos(\omega_a t + \bar{\varphi}_0 + \bar{\varphi}' t) = \cos[(\omega_a + \bar{\varphi}') t + \bar{\varphi}_0]$
 \Rightarrow fit result for ω_a is biased when muon sample phase varies in the fit time window
- ▶ note: muon loss phase effect is different and additional to muon loss effect on positron rate

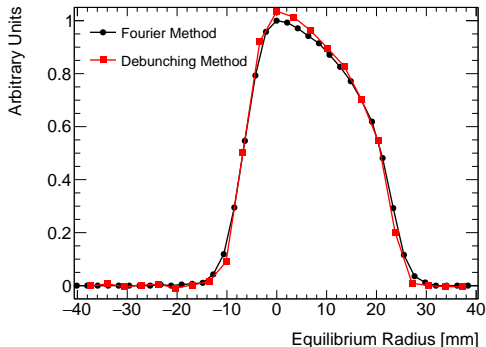
other early to late effects

- ▶ variation of calorimeter gain (corrected before the wiggle plot fit)
- ▶ variation of pileup (proportional to $[N(t)]^2$, corrected before the wiggle plot fit)
- ▶ variation of beam average position and size (phase acceptance)
- ▶ variation of magnetic field due to electric quadrupoles plates vibration
- ▶ variation of magnetic field due to kicker eddy currents

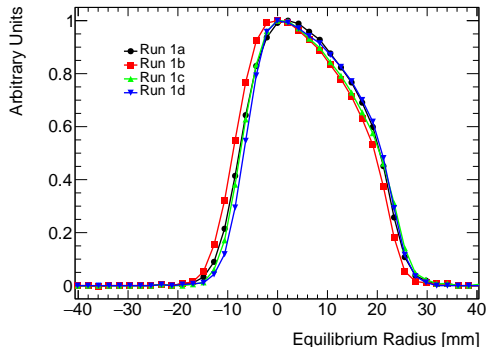
Electric field correction $C_e = +489 \pm 53$ ppb

- ▶ compute momentum distribution from electrons detected at early times after injection
 - ▶ using cosine Fourier transform of rate vs. time
 - ▶ measuring change of shape of rectangular bunches (debunching)
- ▶ compute radial muon distribution from momentum distribution
- ▶ compute electric field contribution to ω_a due to quadrupoles electric field

cosine Fourier vs. debunching method



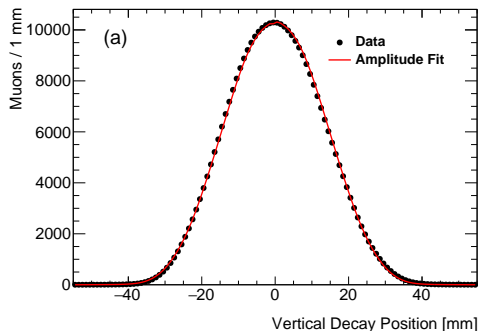
radial distributions in the four datasets



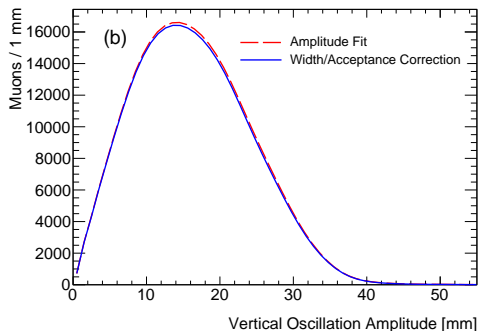
$$\text{Pitch correction } C_p = +180 \pm 13 \text{ ppb}$$

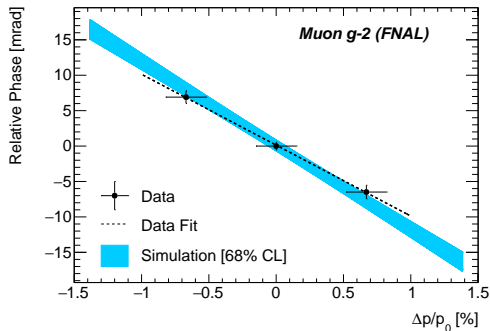
- ▶ reconstruct muon vertical position from decay electrons measured on trackers
- ▶ compute corresponding pitch correction to ω_a

vertical decay vertices distribution

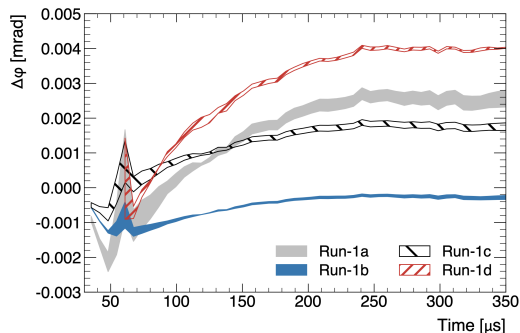


vertical oscillation amplitude distribution



Lost muons phase-variation effect correction $C_{ml} = -11 \pm 5$ ppbmeasured and simulated $\varphi - p$ correlation

- ▶ $d\varphi/dp$ measured on dedicated runs by varying magnetic field by -0.68% , $+0.68\%$
- ▶ measurement consistent with simulation

estimated $\Delta\varphi(t)$ due to muon loss

- ▶ use delivery ring collimators to change the muon momentum distribution
- ▶ muon loss function of time and momentum fitted using simulation-inspired analytic function to model observed beam loss for different muon momentum distributions

Phase-Acceptance correction $C_{pa} = -158 \pm 75$ ppb

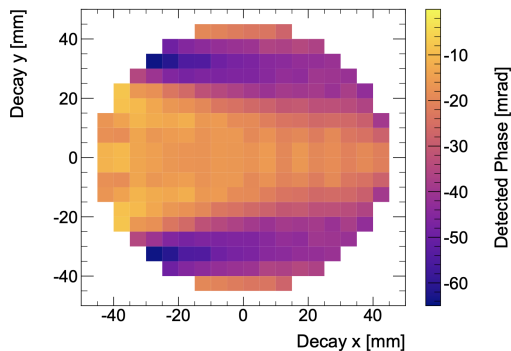
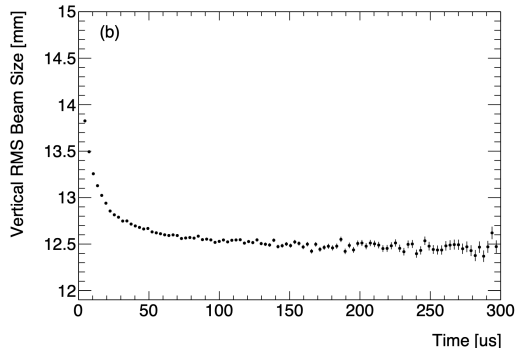
▶ effective phase variation due to variation of beam horizontal and vertical position and spread

▶ example: $\Delta\omega_a = \frac{d\varphi}{dt} = \frac{d\varphi}{dY_{RMS}} \cdot \frac{dY_{RMS}}{dt}$

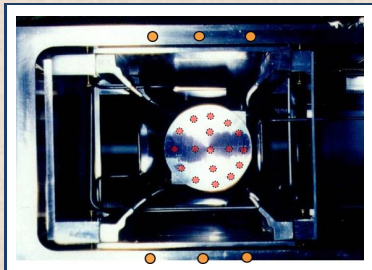
▶ obtained with simulation

▶ measured with trackers and extrapolated to whole ring with beam dynamics simulations

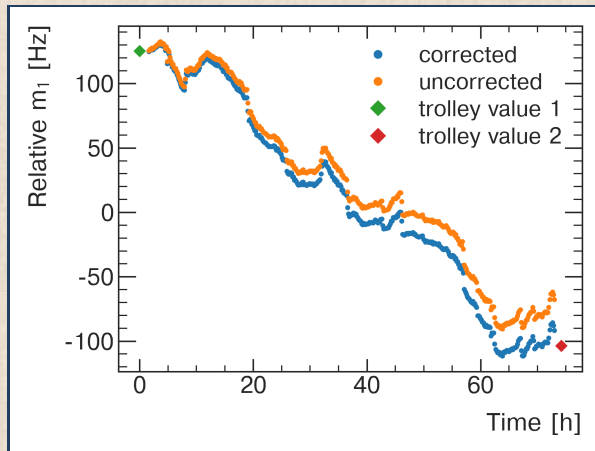
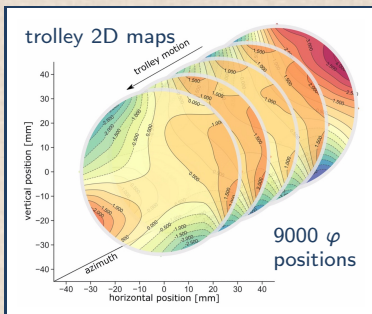
phase as a function of muon position

variation of Y_{RMS} 

Measuring ω_p / magnetic field with fixed and trolley probes



- ▶ 378 fixed probes measure continuously the magnetic field
- ▶ 17-probes trolley run along muons path every ~ 3 days
- ▶ fixed probes measurements corrected using trolley measurements



Measuring ω_p magnetic field: calibration of probes

calibration

- ▶ each trolley probe calibrated with **absolute cylindrical probe** placed in the same position inside the storage ring
- ▶ absolute cylindrical probe calibrated to reference **absolute spherical probe** in MRI magnet at Argonne National Laboratory
- ▶ absolute spherical probe consistent with novel absolute ^3He probe
- ▶ 17 probes calibration uncertainty 20 – 48 ppb

reference temperature

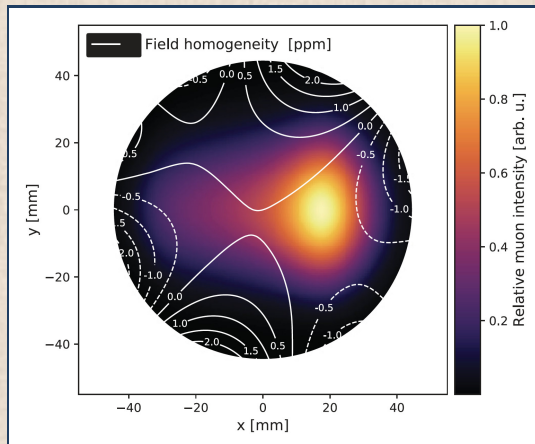
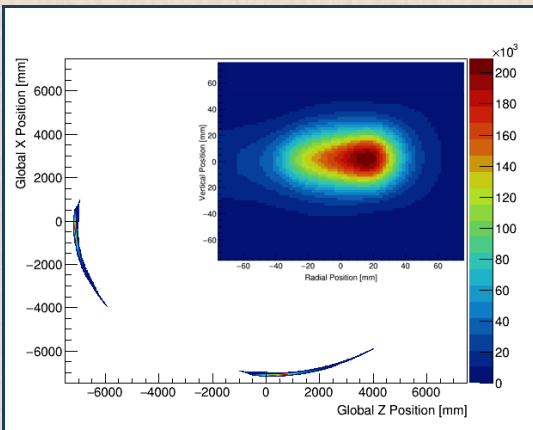
- ▶ magnetic field measurements corrected to be expressed as $\omega'_p(T)$, precession frequency of shielded proton spin in spherical water sample at reference temperature of 34.7 °C

absolute spherical probe



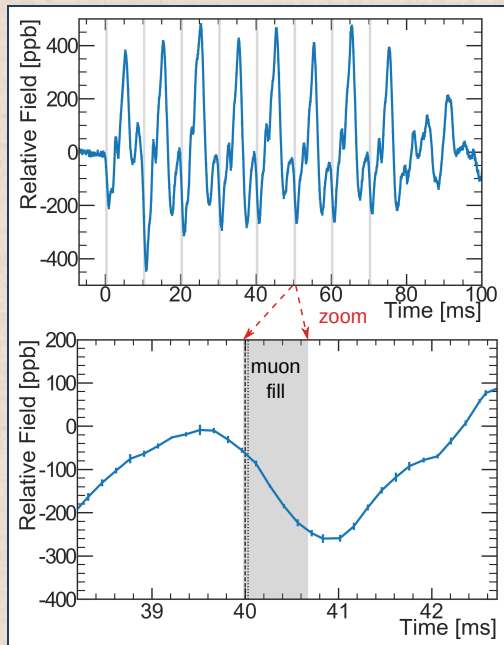
$\tilde{\omega}'_p(T)$ (magnetic field experienced by the muons) measured to 56 ppb

- ▶ tracker reconstructs muons decay vertices in parts of storage region
- ▶ beam dynamics simulation used to extrapolate to whole storage region
- ▶ magnetic field map averaged over muon distribution
- ▶ two independent groups did the measurement, one additional group the calibration



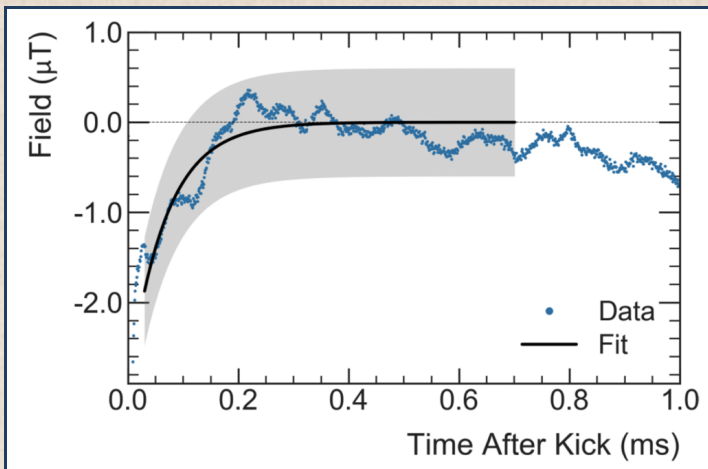
Electric quadrupoles transient field correction $B_q - 17 \pm 92$ ppb

- ▶ electric quadrupoles are pulsed (to prevent static charge accumulation)
- ▶ plates vibration perturbs magnetic field
- ▶ special NMR probes measure the transient field perturbation in muon region
- ▶ large uncertainty because mapping incomplete will improve in Run 2+



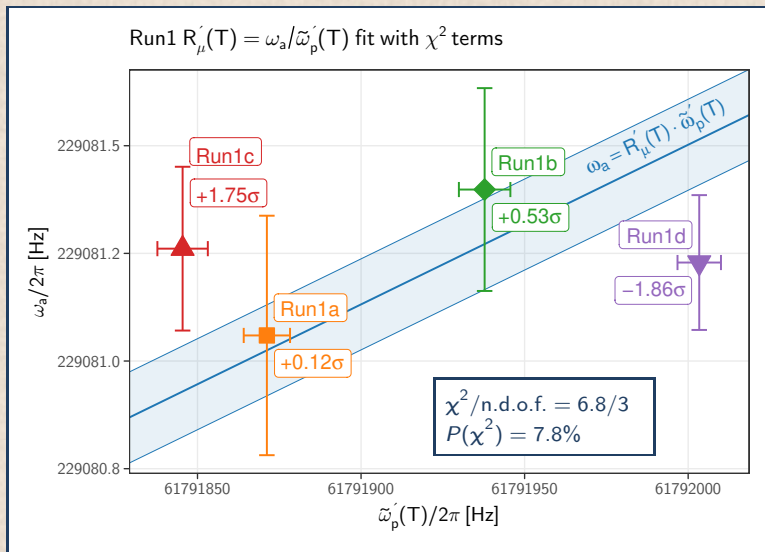
Kicker magnets transient field correction $B_k = -27 \pm 37$ ppb

- ▶ kicker magnets pulsed before start of fit window
- ▶ induced eddy currents perturb magnetic field inside fit window
- ▶ magnetic field perturbation measured with a Faraday effect magnetometer



All corrections and uncertainties estimated before unblinding

	Correction	Uncertainty	Design goal
ω_a^m (statistical)	–	434	100
ω_a^m (systematic)	–	56	
base clock	–	2	
C_e	489	53	
C_p	180	13	
C_{ml}	-11	5	
C_{pa}	-158	75	
ω_a beam dynamics corrections ($C_e + C_p + C_{ml} + C_{pa}$)	499	93	
ω_a total systematic	499	109	70
$\omega_p'(T)(x, y, \varphi)$	–	54	
$M(x, y, \varphi)$	–	17	
$\langle \omega_p'(T)(x, y, \varphi) \times M(x, y, \varphi) \rangle$	–	56	
B_q	-17	92	
B_k	-27	37	
$\tilde{\omega}_p'(T)$ transient fields corrections ($B_q + B_k$)	-44	99	
$\tilde{\omega}_p'(T)$ total [note: correction sign now for $\omega_a/\tilde{\omega}_p'(T)$]	44	114	70
$\omega_a/\tilde{\omega}_p'(T)$ total systematic	544	157	100
external measurements	–	25	
total [correction is for $\omega_a/\tilde{\omega}_p'(T)$]	544	462	140

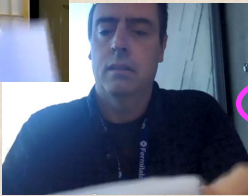
Check consistency of $R'(T) = \omega_a/\tilde{\omega}'_p(T)$ for the four Run 1 datasets

► reported χ^2 terms are larger than one can guess on the χ^2 plot because uncertainties are partly correlated

Unanimous consensus for unblinding in a remote collaboration meeting



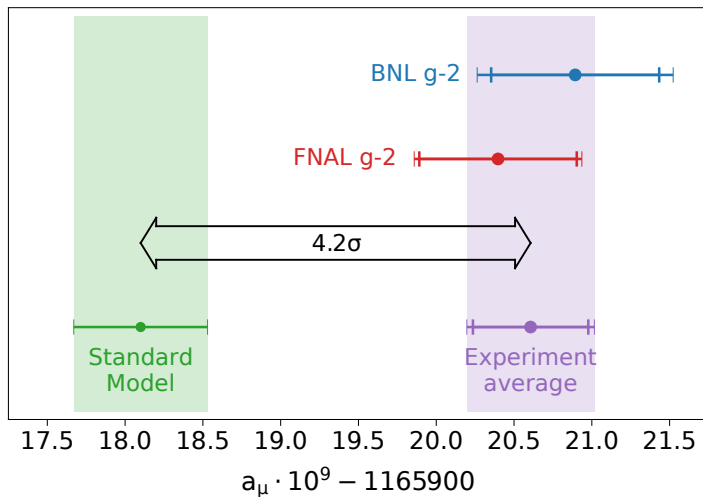
UW envelope



FNAL envelope

g-2 blinding numbers
2999 8956
3999 7844



First FNAL Muon $g-2$ result

+3.66 σ , E821
 $1165920.893(630) \cdot 10^{-9}$

+3.33 σ , E989 Run 1
 $1165920.397(539) \cdot 10^{-9}$

+4.22 σ , E989 Run 1 + E821
 $1165920.607(410) \cdot 10^{-9}$

Muon $g-2$ theory initiative
 $1165918.100(430) \cdot 10^{-9}$

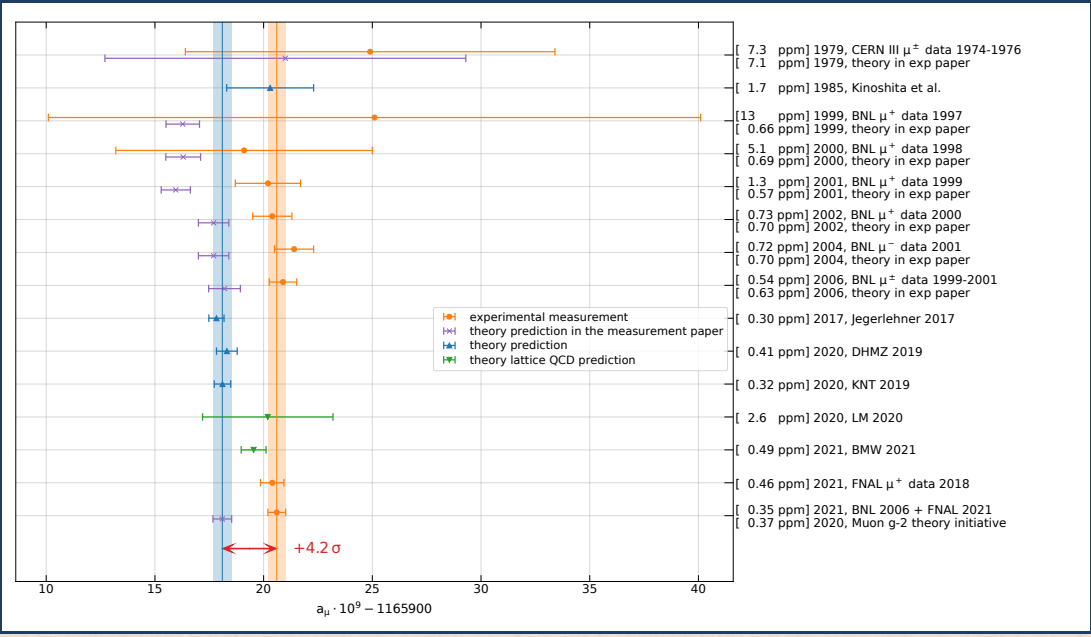
- ▶ $a_\mu(\text{BNL})$ recomputed from $R_\mu(\text{BNL})$ like $a_\mu(\text{FNAL})$
- ▶ included correlation due to external measurements, assumed no other correlation between BNL and FNAL

Three papers published on April 7, 2021, a fourth one accepted



- ▶ Measurement of the Positive Muon Anomalous Magnetic Moment to 0.46 ppm
[doi:10.1103/PhysRevLett.126.141801](https://doi.org/10.1103/PhysRevLett.126.141801)
- ▶ Measurement of the anomalous precession frequency of the muon in the Fermilab Muon $g-2$ Experiment
[doi:10.1103/PhysRevD.103.072002](https://doi.org/10.1103/PhysRevD.103.072002)
- ▶ Magnetic Field Measurement and Analysis for the Muon $g-2$ Experiment at Fermilab
[doi:10.1103/PhysRevA.103.042208](https://doi.org/10.1103/PhysRevA.103.042208)
- ▶ Beam dynamics corrections to the Run-1 measurement of the muon anomalous magnetic moment at Fermilab
[doi:10.1103/PhysRevAccelBeams.24.044002](https://doi.org/10.1103/PhysRevAccelBeams.24.044002)

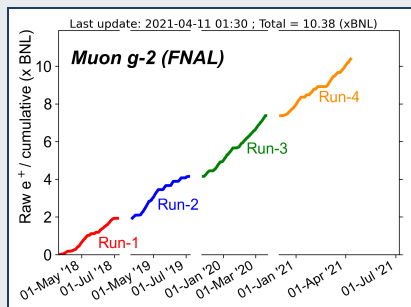
New lattice QCD a_μ prediction (BMW 2021) published on 7 April 2021



What comes next

FNAL-E989 experiment

- ▶ Run 1 is 6% of design goal sample
- ▶ measurement using Run 2+3 data in ~ 1 year



J-PARC Muon $g-2$ /EDM experiment

- ▶ data-taking planned to start in 2024

Muon $g-2$ theory initiative

- ▶ review BMW 2021 lattice QCD prediction
- ▶ new $\sigma(e^+e^- \rightarrow \text{hadrons})$ measurements coming

New Physics models

- ▶ a_μ measurement provides improved constraints on New Physics modes and an improved experimental reference for selecting how NP models rank in fitting all observations

MuonE experiment

- ▶ measures t-channel $\mu - e$ scattering to compute HVP a_μ contribution

Backup Slides

Measurement formula in more detail

$$a_\mu = \left[\frac{\omega_a}{\tilde{\omega}'_p(T)} \right] \cdot \left[\frac{\mu'_p(T)}{\mu_e(H)} \right] \left[\frac{\mu_e(H)}{\mu_e} \right] \left[\frac{m_\mu}{m_e} \right] \left[\frac{g_e}{2} \right]$$

(equivalent to $a_\mu = \frac{\omega_a/\omega_p}{\mu_\mu/\mu_p - \omega_a/\omega_p}$ using CODATA constants)

measurements by the Muon $g-2$ collaboration

- ▶ ω_a precession of muon spin relative to momentum rotation in magnetic field
- ▶ $\tilde{\omega}'_p(T)$ precession frequency of shielded proton spin in spherical water sample at $T = 34.7^\circ\text{C}$ in muon-beam-weighted magnetic field, $\tilde{\omega}'_p(T) = \langle \omega'_p(T)(x, y, \varphi) \times M(x, y, \varphi) \rangle$

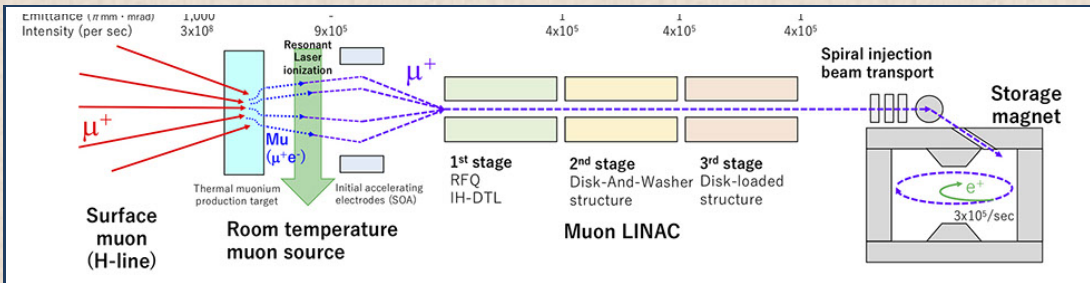
notation

- ▶ $\mu'_p(T)$ magnetic momentum of proton in spherical water sample at 34.7°C
- ▶ $\mu_e(H)$ magnetic momentum of electron in hydrogen atom

external measurements

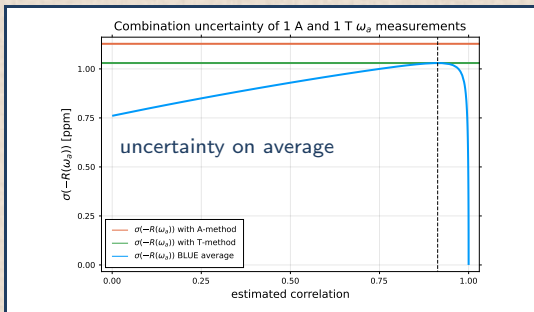
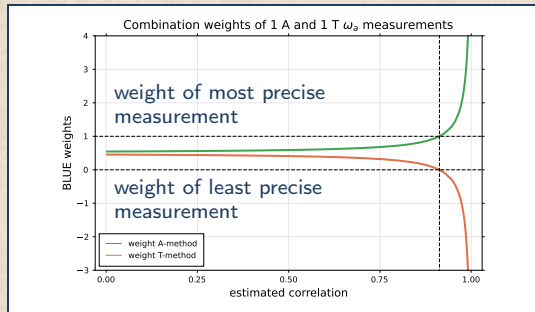
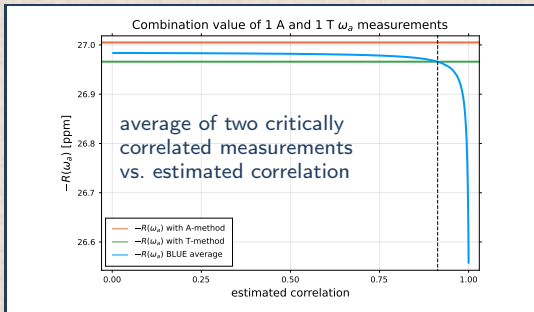
- ▶ $\mu'_p(T)/\mu_e(H)$ 10.5 ppb precision, *Metrologia* 13, 179 (1977)
- ▶ $\mu_e(H)/\mu_e$ 5 ppq (negligible) theory QED calculation, *Rev. Mod. Phys.* 88 035009 (2016)
- ▶ m_μ/m_e 22 ppb precision CODATA 2018 fit, primarily driven by LAMPF 1999 measurements of muonium hyperfine splitting, *Phys. Rev. Lett.* 82, 711 (1999)
- ▶ $g_e/2$ 0.28 ppt (negligible), *Phys. Rev. Lett.* 100, 120801 (2008)

Muon g-2/EDM experiment at J-PARC



- ▶ 50% polarized 300 MeV muons
- ▶ small 3.0 T magnet
- ▶ no electric field, low focusing magnetic field
- ▶ silicon tracker instead of calorimetry
- ▶ $5.7 \cdot 10^{11}$ reconstructed electrons
- ▶ 0.45 ppm statistical uncertainty goal

Critical correlation: $C_{ij}^{\text{crit}} = \rho^{\text{crit}} = \min(\sigma_i, \sigma_j) / \max(\sigma_i, \sigma_j) \quad (i \neq j)$



Least χ^2 average of 2 meas. around $\rho = \rho^{\text{crit}}$

- ▶ unstable vs. value of estimated correlation ρ
- ▶ Glen Cowan, Stat. Data Analysis, sec. 7.6.1
- ▶ Valassi & Chierici 2014, EPJC 74 (2014) 2017
- ▶ but no literature really appropriate for our case

ω_a^m staged A-method average for measurements on same dataset

- ▶ A-method statistically optimal for ideal measurement with only Poisson uncertainties
- ▶ in Run 1 we are close to these conditions because Poisson statistical uncertainties dominate
- ▶ in this approximation, optimal combination = average the (most precise) A-method measurements
- ▶ \Rightarrow combine just the 4 A-method measurements with equal weights, for each dataset
 - ▶ but, taking into account that there is some decorrelation due to using two reconstructions
 - \Rightarrow average first A-measurements using the same reconstruction, then average across reconstructions

ω_a^m uncertainties

	[ppb]
total uncertainty	437
statistical	434
systematics	56
- Time randomization	9
- Gain	8
- Pileup	35
- Muon Loss	3
- CBO	38
- Early to late effect	17

Main ω_a measurement systematics mentioned in E989 TDR

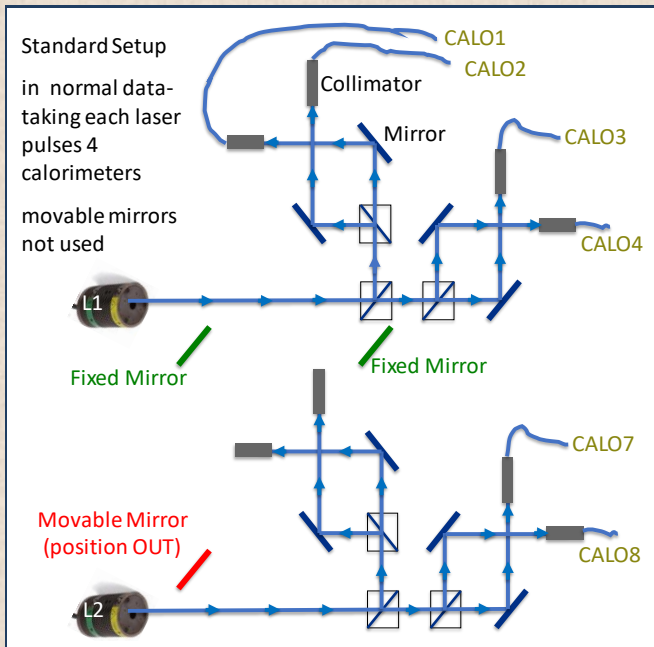
	E821 [ppb]	E989 improvement plans	goal [ppb]	Run 1 [ppb]
gain changes	120	better laser calibration low-energy threshold	20	20
pileup	80	low-energy samples recorded calorimeter segmentation	40	35
lost muons	90	better collimation in ring	20	5
CBO	70	higher n value (frequency) better match of beamline to ring	<30	38
E and pitch	50	improved tracker precise storage ring simulation	30	55
total	180		70	109

Beam dynamics frequencies

			f [MHz]	T [μ s]
Anomalous precession	f_a		0.2291	4.3649
Cyclotron	f_c		6.7024	0.1492
Horizontal betatron	f_x	$= f_c \sqrt{1 - n}$	6.2874	0.1590
Vertical betatron	f_y	$= f_c \cdot \sqrt{n}$	2.3218	0.4307
Coherent betatron oscillation	f_{CBO}	$= f_c - 1 \cdot f_x$	0.4150	2.4097
Vertical oscillation	f_{VO}	$= f_c - 1 \cdot f_y$	4.3806	0.2283
Vertical waist	f_{VW}	$= f_c - 2 \cdot f_y$	2.0589	0.4857

field index $n = 0.12$

2 laser pulses arbitrarily close in time using two laser sources



2 laser pulses arbitrarily close in time using two laser sources

